# Seasonal Dependence of the Global Ionospheric Electric Field Generated by Thunderstorms

Valery V. Denisenko[1], Michael J. Rycroft[2]

[1] Institute of Computational Modelling SB RAS, Krasnoyarsk, Russia

[2] CAESAR Consultancy, Cambridge, UK

A model for the distribution of the ionospheric electric potential which drives the currents which close the currents to the ionosphere generated by thunderstorms and fair weather currents is constructed.

The designed model contains the ionospheric equatorial electrojets up to 160 A at night-time in January.

This investigation is performed with the financial support of the Russian Science Foundation, Grant No. 22-27-00006.

# 1 The Current Continuity Equation

The basic equations for the steady state electric field $\mathbf{E}$ and current density $\mathbf{j}$

$$\operatorname{curl}\mathbf{E} = 0, \quad \operatorname{div}\mathbf{j} = Q, \quad \mathbf{j} = \hat{\sigma}\mathbf{E}, \tag{1}$$

$\hat{\sigma}$ - the conductivity tensor, $\mathbf{j}_{ext}$ - external current density,
$Q = -\operatorname{div}\mathbf{j}_{ext}$
Electric potential $V$, $\mathbf{E} = -\operatorname{grad}V$.
Current continuity equation

$$-\operatorname{div}(\hat{\sigma}\operatorname{grad}V) = Q. \tag{2}$$

Spherical geomagnetic coordinates $r, \theta_m, \varphi_m$, geomagnetic latitude $\lambda_m = \pi/2 - \theta_m$, height above mean sea level $h$.

## 2 Separation of Ionospheric and Atmospheric Conductors

The Earth's ground is an ideal conductor

$$V|_{h=h_g(\theta,\varphi)} = -V_0, \tag{3}$$

the value of the constant $V_0$ will be defined later.

Our model of the topography (Denisenko, Yakubailik, 2015). We define the boundaries separating the ionosphere:

Atmosphere below $h_{_I} = 90$ km

Magnetosphere above $h_{_M} = 500$ km, nonzero conductivity across **B** only in plasma sheet and cusps.

The whole magnetic field line in the ionosphere and magnetosphere is an equipotential object - 2-D model.

Domain decomposition.

## 3 Atmospheric Conductor

Dirichlet boundary value problem (2-4) for the atmosphere that is simulated as a conductor between two ideal conductors:

$$V|_{h=h_I} = 0, \quad V|_{h=h_g(\theta,\varphi)} = -V_0. \tag{4}$$

Because of the large horizontal scale we use the flat 1-D model instead of the 3-D equation

$$-\frac{d}{dh}\left(\sigma(h)\frac{d}{dh}V(h)\right) = 0, \quad V|_{h=h_0} = 0, \quad V|_{h=h_g(\theta,\varphi)} = -V_0.$$

The value $V_0$ is taken to balance the total fair weather and thunderstorm currents.

The conductance of the atmospheric vertical column with $1\,\mathrm{m}^2$ cross-section between ground and ionosphere

$$1/\Sigma(\theta,\varphi) = \int_{h_g(\theta,\varphi)}^{h_0} dh \,/\, \sigma(h). \tag{5}$$

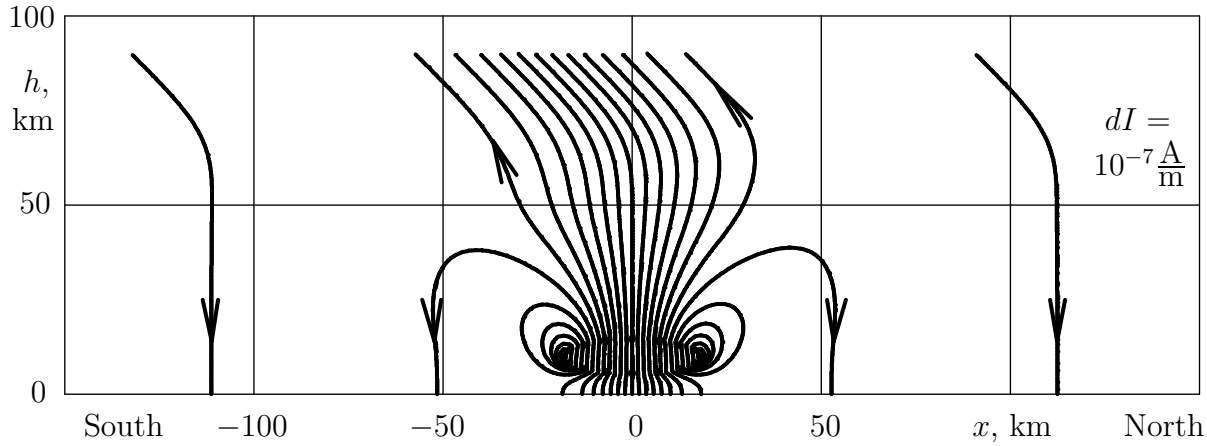


Fig. 1. The current lines for the total current in the neighborhood of a thunderstorm cloud.

The model of the global distribution of thunderstorms (Denisenko and Lyakhov, 2021) obtained from the ground-based World Wide Lightning Location Network (WWLLN).

Lightnings are used as proxy for thunderstorm current to the ionosphere, normalized with Carnegie data.

## Carnegie data in (UT, months) coordinates

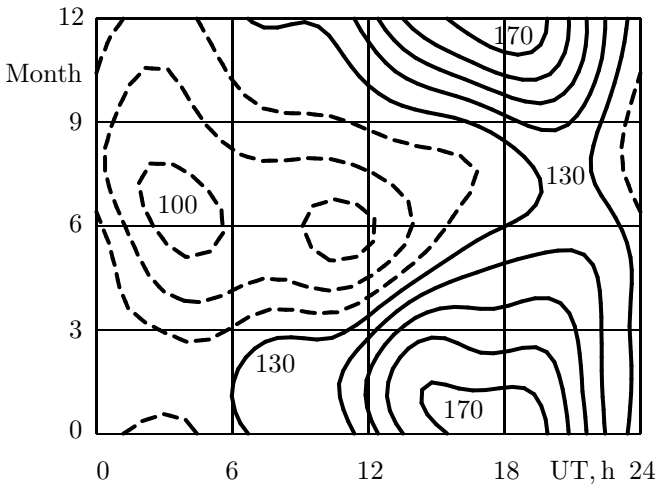


Fig. 2. The vertical electric field above the ocean surface derived from the Carnegie Cruise VII data. Contours of $E_0$ with intervals of 10 V/m. Dashed lines for $E_0 \leq 120$ V/m.

January, 18 UT, Empirical model of height distributions of $\sigma(h)$;
$E_0 = 177$V/m above ocean by Carnegie plot;
$E_0 = 260$V/m and current density $j_0 = 5\text{pA/m}^2$ above ground;
total current of GEC 2800 A;
ground-ionosphere voltage $V_0 = 500$kV.

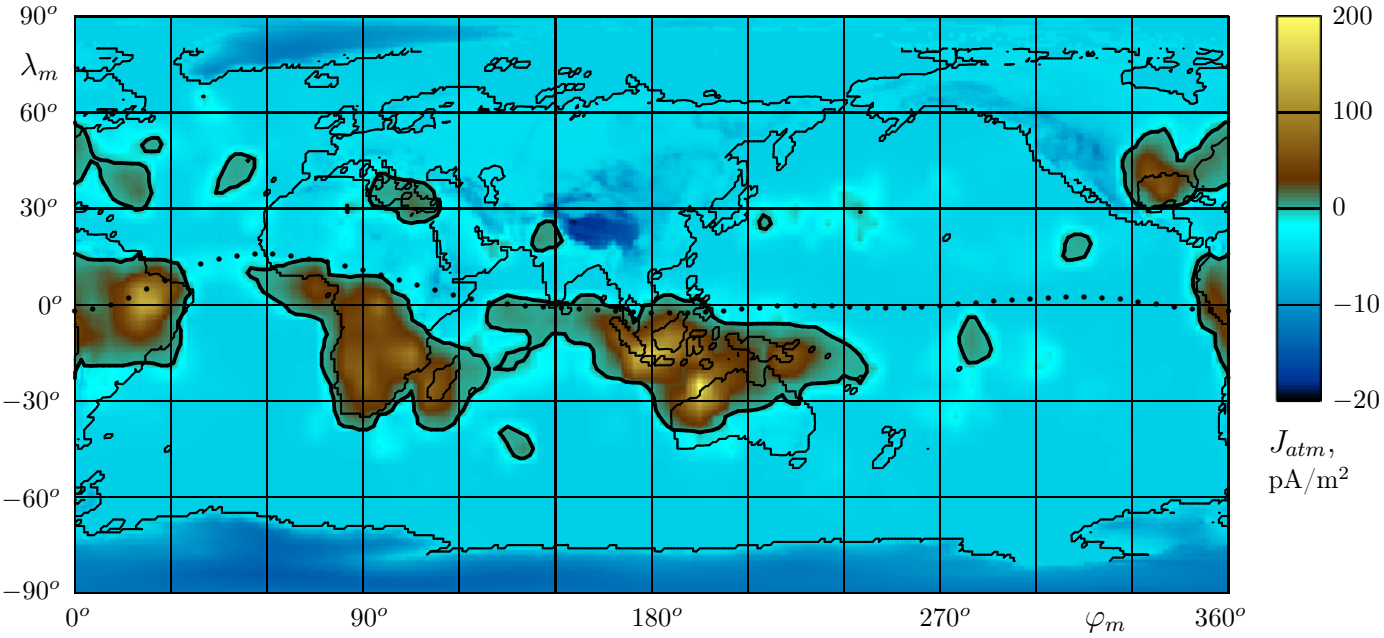


Fig. 3. The global distribution of thunderstorm currents to the ionosphere summed with the fair weather currents. January, 18 UT. Obtained in (Denisenko, Lyakhov, 2021) by WWLLN data. Different linear color scales for positive and negative current density. The bold contours separate thunderstorm regions $J_{atm} > 0$.

## 5 Conductivity in the Earth's Ionosphere

We use parallel and normal to the direction of magnetic induction $\mathbf{B}$ components of vectors which are marked with symbols $\parallel$ and $\perp$. Ohm's law (1) in a gyrotropic medium

$$j_{\parallel} = \sigma_{\parallel} E_{\parallel}, \qquad \mathbf{j}_{\perp} = \sigma_{P} \mathbf{E}_{\perp} - \sigma_{H} \left[\mathbf{E}_{\perp} \times \mathbf{B}\right] / B, \tag{6}$$

Hall ($\sigma_H$), Pedersen ($\sigma_P$), field-aligned ($\sigma_{\parallel}$) conductivities. They are calculated using the empirical models IRI, MSISE, IGRF.

2-D model, Pedersen and Hall conductances $\Sigma_P, \Sigma_H$:

$$\mathbf{J}_{\perp} = \begin{pmatrix} \Sigma_P & \Sigma_H \\ -\Sigma_H & \Sigma_P \end{pmatrix} \mathbf{E}_{\perp}, \tag{7}$$

$$\Sigma_P = \int \sigma_P \, dl, \qquad \Sigma_H = \int \sigma_H \, dl. \tag{8}$$

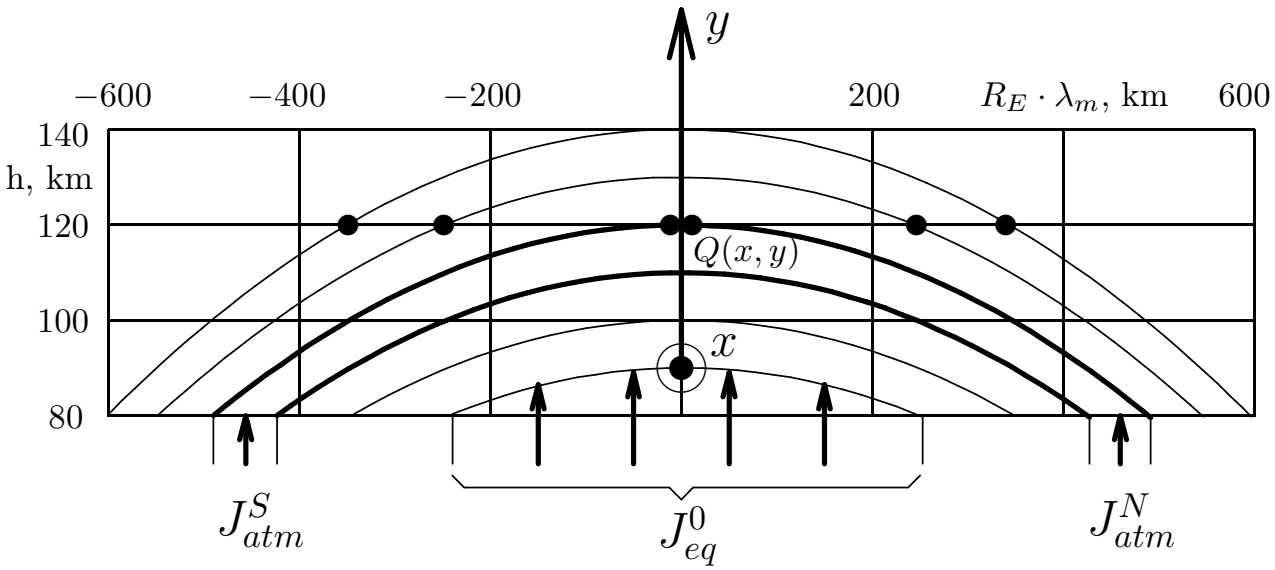


Fig. 4. Magnetic field lines in the ionospheric layer for $\varphi_m = 270^o$. Bold straight segment show the cross-sections of the reference domain with Cartesian coordinates (the x-axis looks to us) which are used in 2-D model.

The charge conservation law in some plane with Cartesian coordinates $x, y$ that presents all magnetic field

$$-\frac{\partial}{\partial x}\left(\Sigma_{xx}\frac{\partial V}{\partial x}+\Sigma_{xy}\frac{\partial V}{\partial y}\right)-\frac{\partial}{\partial y}\left(\Sigma_{yx}\frac{\partial V}{\partial x}+\Sigma_{yy}\frac{\partial V}{\partial y}\right)=Q_{ext}, \quad (9)$$

$Q_{ext}$ - the density of current from the atmosphere, transformed to the new coordinates $x, y$. The partial differential equation (9) is an equation of elliptical type.

The main part contains middle- and low latitudes:

$$V|_{\Gamma_{aur}}=0, \quad J_\nu|_{\Gamma_{eq}}=-J^0_{eq}, \quad (10)$$

where the boundary $\Gamma_{aur}$ is in the auroral zones, $\Gamma_{eq}$ corresponds to the last magnetic field lines which are regarded as ionospheric ones.

Our numerical method for the boundary value problem (9, 10) is described in detail in (Denisenko, 1998).

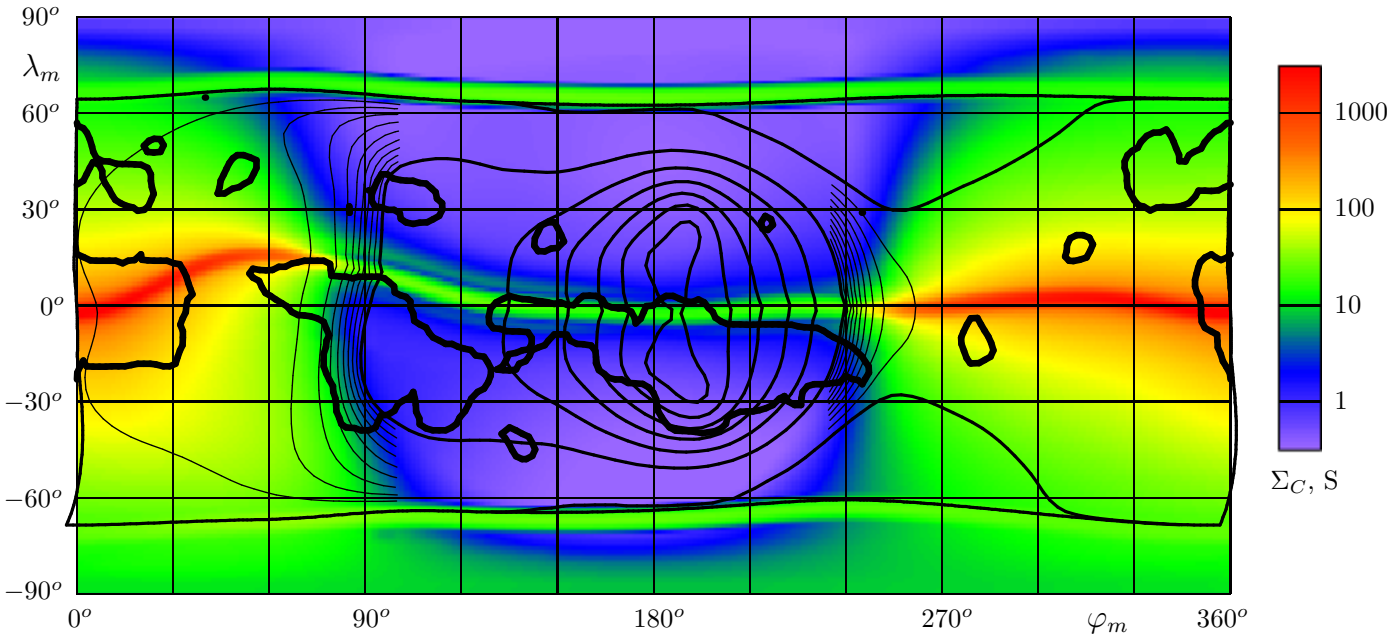


Fig. 5. Distribution of the Cowling conductance $\Sigma_C$ for January, 18 UT.

The bold contours separate thunderstorm regions $J_{atm} > 0$.

Equipotentials are plotted with contour interval of 50 V. Additional equipotentials are plotted 10 times more often as thin lines.

## 7 The Results of the Calculations

In the well known model (Hays, Roble, 1979) the ionospheric conductances were principally simplified as $\Sigma_H \equiv 0$ and $\Sigma_P \equiv 0.05\,\mathrm{S}$. The maximum potential difference within the ionosphere was 1575 V.

Our model gives 5 times less voltage even in the extremal case: January, 18 UT, low solar activity.

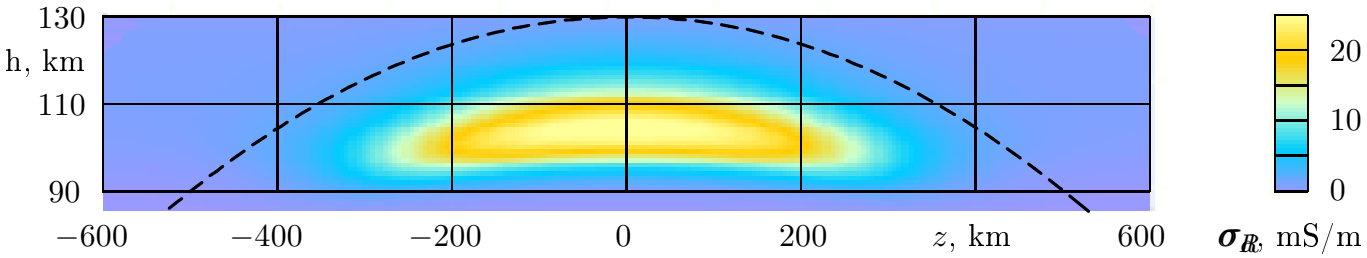


Fig. 6. A night-time cross-section of the electrojet, $\sigma_R(z,h)$.

$$j_\varphi = \sigma_R E_\varphi, \quad \sigma_R = \sigma_P + \sigma_H \Sigma_H / \Sigma_P, \quad \Sigma_C = \int \sigma_R \, dl$$

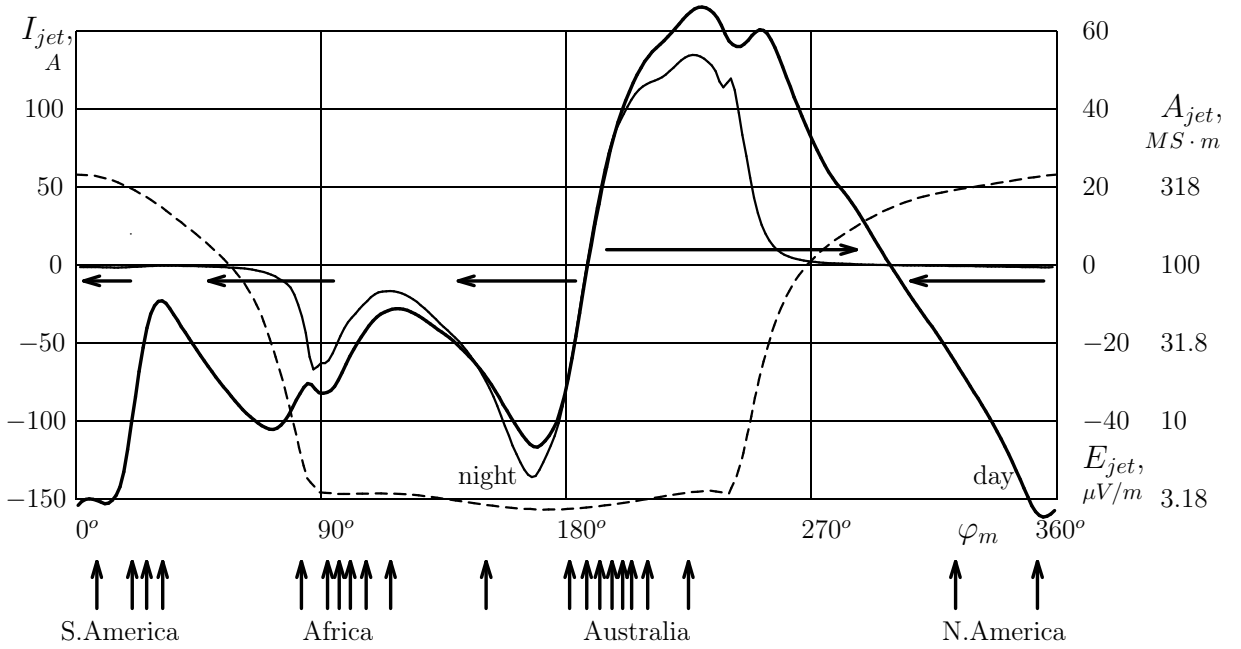


Fig. 7. The current of the electrojets $I_{jet}(\varphi_m)$ (bold line), the electric field component $E_{jet}(\varphi_m)$ (thin line), the conductance of the electrojet area $A_{jet}(\varphi_m)$ on a logarithmic scale (dashed line).

Vertical arrows mark the currents to the ionosphere from the thunderstorms; each arrow means 100 A near that meridian.

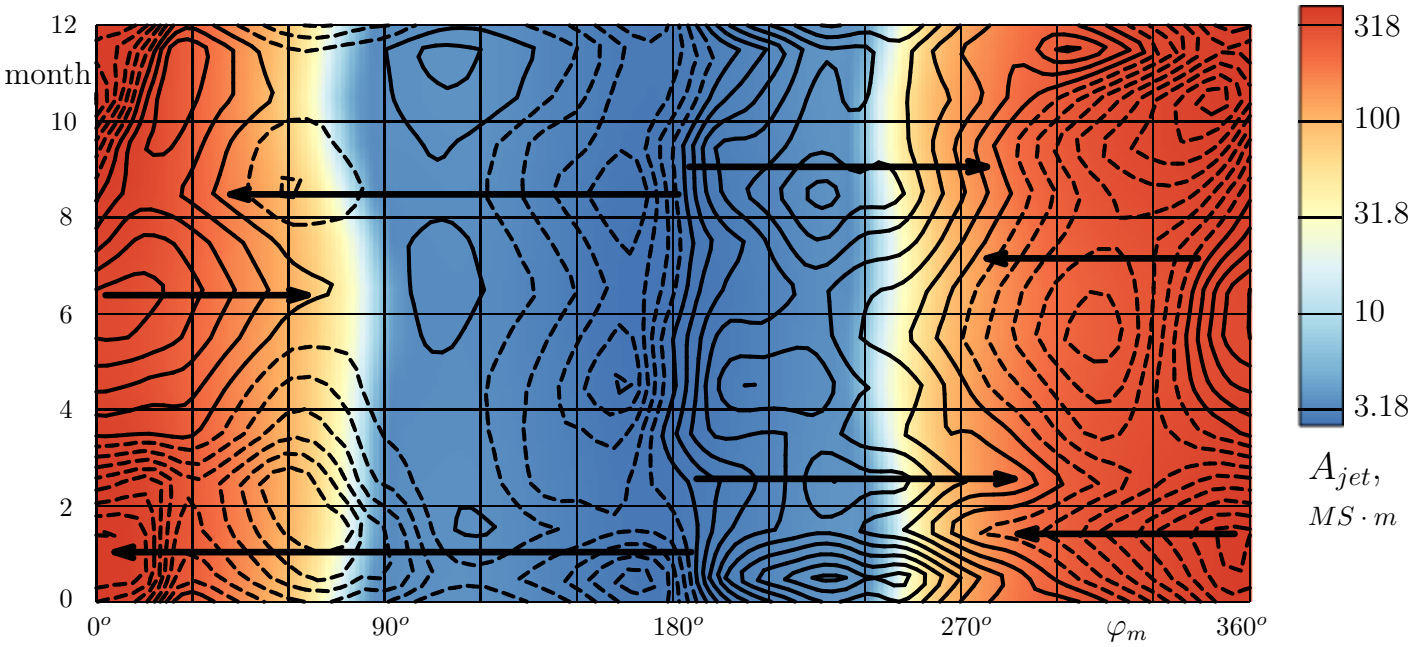


Fig. 8. Seasonal variations of the electrojets $I_{jet}(\varphi_m)$ at 18 UT. Contours are plotted with interval of 20 A. Dashed lines for $I < 0$ (westward currents). Arrows show the directions of the electrojets.

The conductance of the electrojet area $A_{jet}(\varphi_m)$ is shown with color scale. It equals to the integral of the Cowling conductance.

## 8 Conclusions

The obtained electric field in the ionosphere is an order of magnitude less than that in the model (Hays, Roble, 1979) because of better approach for the simulation of the ionospheric conductivity.

The thunderstorm related part of the GEC contains day- and night-time eastward and westward equatorial electrojets. Currents of these electrojets reaches 160 A in January.

They produce magnetic perturbations in the 0.1 nT range. In principle, they could be measured at the night-time geomagnetic equator where they may not be hidden by electrojets of the global current systems produced by ionospheric and magnetospheric generators.

# Thank you!

## References


[1] Denisenko, V.V.: Multigrid method for a global Hall conductor in the Earth's ionosphere. Virtual Proceedings of the 10-th Anniversary International GAMM - Workshop on Multigrid Methods. (1998) http://www.mgnet.org/mgnet-parmgm98.html

[2] Denisenko, V.V., Biernat, H.K., Mezentsev, A.V., Shaidurov, V.A., Zamay, S.S.: Modification of conductivity due to acceleration of the ionospheric medium. Ann. Geophys. 26, 2111-2130 (2008) doi:10.5194/angeo-26-2111-2008

[3] Denisenko, V.V., Lyakhov, A.N.: Comparison of ground-based and satellite data on spatiotemporal distribution of lightning discharges under solar minimum. Solar-Terr. Phys. 2021. 7(4), 104-112. doi: 10.12737/stp-74202112

[4] Denisenko V.V., Rycroft M.J. The Equatorial Electrojets in the Global Electric Circuit. 2021. Journal of Atmospheric and Solar-Terrestrial Physics. 221(3):105704. Doi: 10.1016/j.jastp.2021.105704

[5] Denisenko, V.V., Rycroft, M.J., Harrison, R.G.: Mathematical Simulation of the Ionospheric Electric Field as a Part of the Global Electric Circuit. Surv. Geophys. 40(1), 1-35 (2019). doi:10.1007/s10712-018-9499-6

[6] Denisenko, V.V., Rycroft, M.J., Harrison, R.G.: Correction to: Mathematical Simulation of the Ionospheric Electric Field as a Part of the Global Electric Circuit. Surv. Geophes. 40(1), 37 (2019) doi: 10.1007/s10712-018-9505-z

[7] Hays, P.B., Roble, R.G.: A quasi-static model of global atmospheric electricity. 1. The lower atmosphere. J. Geophys. Res. 84(A7), 3291-3305 (1979) doi:10.1029/JA084iA07p03291

[8] Richmond, A.D.: Equatorial electrojet. 1. Development of a model including winds and instabilities. J. Atmos. Terr. Phys. 3(6), 1083-1103 (1973).